Three-body coupling in electron-hydrogen ionizing collisions

Jamal Berakdar
Atomic and Molecular Physics Laboratories, Research School of Physical Sciences and Engineering, Australian National University, Canberra, Australian Capital Territory 0200, Australia
(Received 10 April 1996)

In this work a method is established for isolating effects due to single or successive two-body scatterings from those arising from three-body coupling in a three-particle Coulomb system above the complete breakup threshold. It is shown that three-body interactions decide the weighting of individual scattering amplitudes, and hence, determined the interference pattern of these amplitudes. In addition, the method is applied to the analysis of low-energy, electron-impact ionization of atomic hydrogen in the coplanar asymmetric energy-sharing kinematic. The ionization dynamic leading to the measured cross section is unraveled. It is demonstrated that, unlike the situation at higher energies, at low incident energies the cross section is largely decided by interferences indicating a strong three-body coupling. [S1050-2947(97)01501-1]

PACS number(s): 34.80.Dp, 34.10.+x

It is well established that single or successive two-body (classical) collisions lead, under certain circumstances, to identifiable structures in the cross section in various channels of the few-body Coulomb scattering reaction [1–9]. On the contrary, the manifestation of three-body coupling is much less understood. This is partly due to the fact that, unlike the situation for isolated two-body systems, a rigorous introduction of interactions governing three-body couplings is not obvious. It is the aim of this work to systematically introduce three-body coupling and to provide a scheme for disentangling effects originating from three-body interactions from those essentially due to two-body interactions. The theory is applied to the analysis of electron-impact ionization of atomic hydrogen. The latter scattering system has been investigated in a variety of experimental arrangements. Each collision geometry highlights certain aspects of the ionization dynamics. For moderate and high incident velocities (with respect to the Bohr velocity of the initially bound electron), the ionization process has been thoroughly investigated [10–12,8]. In the coplanar asymmetric energy-sharing kinematic the incident direction lies in the plane spanned by the vector momenta of the outgoing electrons which emerge with significantly different energies. In this case the dominant ionization mechanisms are well understood (see Ref. [8] for a review). A major feature of the cross section is a *binary peak* originating from a single-binary electron-projectile encounter, and a less prominent *recoil peak* which is assigned to a second-order process in which the atomic electron, after being hit by the projectile, recoils off the nucleus via initial binding. Although interference between different scattering amplitudes affects heights and positions of these peaks [13], these structures are manifestations of (sequential) two-body interactions.

In the coplanar doubly symmetric geometry in which the incident direction bisects the mutual emission angle of the two equal-energy electrons, a new structure in the cross section arises at backscattering directions where the two electrons escape perpendicular to each other. The appearance of this peak is due to a double-scattering Thomas process where the projectile collides with the atomic electron after recoiling off the nucleus [14]. The latter process is described essentially by sequential two-body interactions. At lower impact energies, the backscattering peak is considerably enhanced. In Ref. [15] it has been shown that adding an *ad hoc* initial-state polarization potential results in an enhanced backscattering peak. At lower excess energies the electron-impact ionization of atomic hydrogen has been theoretically and experimentally investigated exclusively in the equal-energy sharing geometry.

In this work we present a theoretical analysis of electron-impact ionization of atomic hydrogen in coplanar asymmetric energy-sharing kinematic at an excess energy as low as 13.6 eV. Surprisingly, the measured angular distribution of the slow electrons resembles the case of high incident energy, i.e., a binary plus recoil peaks structure. This could lead to the conclusion that (classical) sequential two-body-collision processes, as described above, are the dominant ionization mechanisms. In other words, three-body coupling is marginal in this situation. As shown below, however, this behavior of the measured cross section is illusionary as three-body coupling largely determines the observed cross section. Their manifestation, however, resembles effects originating from two-particle interactions. To establish this conclusion and to isolate three-body effects from two-body effects, we develop a cluster model of a general three-body Coulomb scattering reaction in which the three-particle system is broken down into three, noninteracting two-body subsystems which are subsequently coupled to each other. The strength of the latter coupling determines the extent of the three-body effect. To achieve this we reformulate the three-body time-independent Schrödinger equation with outgoing-wave boundary conditions in the set of coordinates:

$$\{\xi_k = r_{ij} + \hat{\mathbf{k}}_{ij} \cdot \mathbf{r}_{ij}\,; \xi_m = r_{ij}\},$$

$$\epsilon_{ijk} \neq 0; j > i, k \in [1,3]; m \in [4,6]. \tag{1}$$

In Eq. (1) $\hat{\mathbf{k}}_{ij}$ denotes the directions of the momenta $\mathbf{k}_{ij}$, conjugate to the interparticle distances r_{ij}. It has been shown in Ref. [16] that the three-body Hamiltonian H, expressed in the coordinate system (1), splits into two *parametrically* coupled differential operators; an operator $H_{\xi_{1\cdots3}}$ which is

differential in the coordinates $\xi_{1\ldots3}$ only and an operator differential in internal degrees of freedom $r_{ij};j>i\in[1,3]$. An additional mixing term arises from the off-diagonal elements of the metric tensor. The decisive point is that the Hamiltonian $H_{\xi_{1\ldots3}}$ is the sum of three commuting, two-body Coulomb Hamiltonians, i.e., it is exactly separable in the coordinates $\xi_{1\ldots3}$. Thus, within the approximation $H\approx H_{\xi_{1\ldots3}}$, the three-body system is considered as the sum of three spatially decoupled two-body Coulomb systems. The exact regular eigenfunction of $H_{\xi_{1\ldots3}}$ at a given total energy E has the explicit form [16]

$$\begin{aligned}\Psi(\xi_1,\xi_2,\xi_3)|_{(\xi_4,\xi_5,\xi_6)}&=N\exp(i\mathbf{r}_{ij}\cdot\mathbf{k}_{ij}+i\mathbf{R}_k\cdot\mathbf{K}_k)\\&\times{}_1F_1(i\beta_{23}(\xi_4,\xi_5,\xi_6),1,-ik_{23}\xi_1)\\&\times{}_1F_1(i\beta_{13}(\xi_4,\xi_5,\xi_6),1,-ik_{13}\xi_2)\\&\times{}_1F_1(i\beta_{12}(\xi_4,\xi_5,\xi_6),1,-ik_{12}\xi_3).\end{aligned}\tag{2}$$

In Eq. (2) the coordinate $\mathbf{R}_k$ refers to the particle ''k'' with respect to the center of mass of the pair ''ij'' while $\mathbf{K}_k$ designates the momentum conjugate to this coordinate. The Sommerfeld parameters β_{ij} are given by

$$\beta_{ij}=\frac{Z_{ij}(\xi_m)\mu_{ij}}{k_{ij}},\quad m\in[4,6],\tag{3}$$

where the reduced mass of the pair ''ij'' is denoted by μ_{ij}. The parametric dependence of $H_{\xi_{1\ldots3}}$ on the internal coordinates is reflected by the product charges $Z_{ij}(\xi_m)$ being allowed to be functions of the internal coordinates $\xi_{4\ldots6}$ under the constraint that these functions do not alter the Schrödinger equation. This additional freedom allows the introduction of three-body coupling, i.e., coupling of each two-body Coulomb subsystem to the third-charged continuum particle. Thus we assume that the interaction between two continuum particles depends not only on their mutual Coulomb interaction but on the strength of coupling to the third particle, i.e.,

$$V^i=\sum_{j=1}^{3}a_{ij}V^j,\quad i=1,2,3,\tag{4}$$

where $V^k\equiv V_{ij};\epsilon_{ijk}\neq0$ is the Coulomb potential between particles ''i'' and ''j'' and the 3×3 matrix $\mathcal{A}$ with elements $a_{ij}(\xi_{4\ldots6})$ describes the amount of three-body coupling. The matrix elements a_{ij} are subject to the constraint $\Sigma_{j=1}^{3}a_{ij}=1$ which ensures the invariance of $H_{\xi_{1\ldots3}}$, and thus the total Hamiltonian H under the transformation given by Eq. (4). The identity transformation $\mathcal{A}=\mathbb{1}$ fulfills all the requirements on $\mathcal{A}$ but it means that the coupling (in configuration space) between the two-body subsystems is neglected. Hence, three-body coupling is described by the off-diagonal elements of $\mathcal{A}$. The above analysis applies for a general scattering system of three charged particles. The physical and mathematical properties of individual three-body complexes are contained in the matrix $\mathcal{A}$.

For two electrons receding from the nucleus, which is the final state of electron-impact ionization of atomic hydrogen, the matrix elements a_{ij}, which couple the three two-body subsystems to each other, are determined by requiring the wave function, given by Eq. (2), to be an exact eigenfunction of H (with eigenenergy E) on a five-dimensional closed manifold defined by a constant asymptotically large hyperradius [16]. In addition, we require that the wave function Ψ must correctly describe the Wannier ionization mode [17] in which the two electrons escape outward on opposite sides of, and equal distances from, the nucleus. Further, the Wannier threshold law for the dependence of the total cross section on the excess energy at the complete fragmentation threshold should be reproduced when representing the final state by Ψ [18]. The explicit form of $\mathcal{A}$ determined in this way, hereafter denoted by $\mathcal{A}^c$, is given in Ref. [16,18]. The important point for the present work is that by comparing results for observable quantities calculated in case $\mathcal{A}=\mathcal{A}^c$ and $\mathcal{A}=\mathbb{1}$ we can immediately deduce the influence of three-body coupling.

The first example is given in Fig. 1 for the electron-impact ionization of atomic hydrogen in the coplanar asymmetric kinematic at moderate incident energies. As mentioned above, structures observed in the cross section (Fig. 1) are attributed to (successive) two-body interactions. Hence, three-body coupling is expected to be weak in this geometry

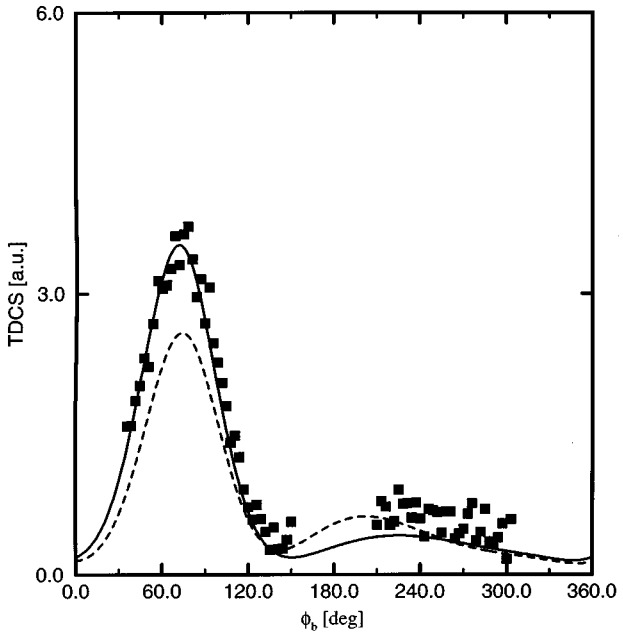

FIG. 1. The triply differential cross section (TDCS) for the electron-impact ionization of atomic hydrogen in the coplanar, asymmetric energy-sharing geometry. The incident energy is 150 eV. The fast scattered electron is detected at an angle of 10^o with respect to the incident direction, whereas the angular distribution of the secondary electron with fixed energy of 5 eV is measured. The emission angle of the latter electron with respect to the incident direction is denoted by Φ_b. The absolute experimental data (full squares) are taken from Ref. [10]. The solid curve represents the results of the model employing $\mathcal{A}=\mathcal{A}^c$ with the approximation that the total potential is conserved along the trajectories of free particles. Results of the model with $\mathcal{A}=\mathbb{1}$ are also depicted (dashed curve).

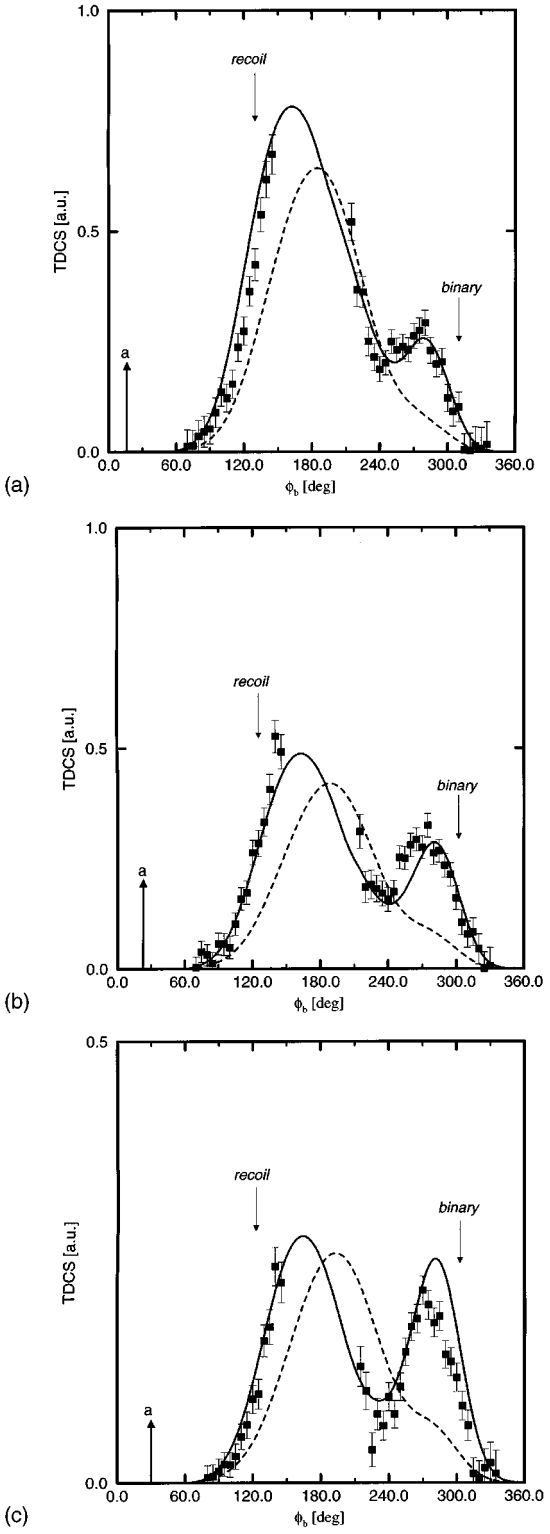

FIG. 2. (a) The same as in Fig. 1; however, the excess energy is chosen as 13.6 eV. The ejected electron possesses an energy of 4 eV. The faster electron is detected at a fixed angle $\Phi_a = 16^o$ with respect to the incident direction (indicated by an arrow). Experiments are courtesy of Ref. [21]. The positions of the binary and recoil peaks are indicated. (b) The same as in (a) but $\Phi_a = 23^o$. (c) The same as in (a) but $\Phi_a = 30^o$. The experimental data in (a)–(c) are simultaneously normalized at one point to theory.

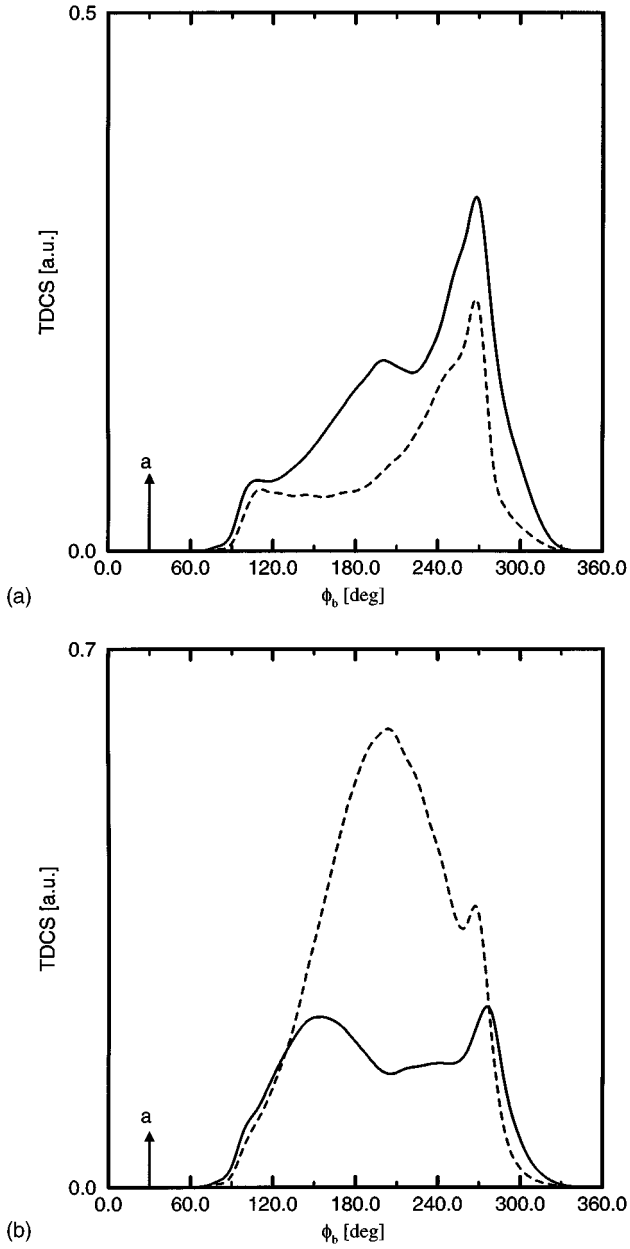

FIG. 3. (a) For the geometry described in Fig. 2(c) the TDCS has been calculated using the projectile-atomic-electron scattering amplitude (T_{ee}) only. (b) Same as in (a) but the projectile-nucleus scattering amplitude (T_{eN}) is employed instead of T_{ee}.

which is confirmed by Fig. 1, although the precise absolute value of the cross section is still sensitive to the interaction details. As the incident energy is decreased [Figs. 2(a)–2(c)] the situation changes dramatically. The theory which disregards three-body coupling ($\mathcal{A}=1$) fails to predict the measured angular pattern whereas the three-body coupled model which employs $\mathcal{A}^c$, correctly reproduces the experimental data. Even though we can now immediately deduce [see Figs. 2(a)–2(c)] the effects of the two-body interactions being distorted by the presence of a third-charged continuum particle, at first glance, the structures prevailing in Figs. 2(a)–2(c) strongly resemble those originating from sequential two-particle collisions. This can be concluded if we consider the two final-state electrons to propagate on the energy shell $E = 13.6$ eV and indicate the positions of the (classical)

binary and recoil peaks [Figs. 2(a)–2(c)], which are essentially due to two-body interactions (see Fig. 1). These positions almost coincide with the observed peaks in the cross section. In particular, the shift in positions can be attributed to the electron-electron final-state repulsion which pushes the secondary electron away from the forward-scattered electron resulting in a backward-squeezed angular distribution of the slower electron.

We are therefore confronted with the questions; how can three-body interactions result in structures which can be interpreted in terms of two-particle scattering on the two-body energy shell and how the observed cross sections are influenced by three-body interactions? The calculations shown in Figs. 3(a) and 3(b) help us answer these questions. We first remark that the direct-scattering amplitude provides the major contribution to the spin-averaged cross section, i.e., the indistinguishability of the two electrons plays a minor role in determining the shape of the angular distribution (although the spin asymmetry shows a rapid variation [19]). Upon inspection of the incoherent contributions of the individual scattering amplitudes, i.e., scattering from the nucleus T_{eN} [Fig. 3(b)] and scattering from the atomic electron T_{ee} [Fig. 3(a)] we can deduce that the peaks in the angular distribution of T_{eN} and T_{ee} are largely decided by two-body interactions. That means, the direct electron-electron scattering gives rise to the binary peak indicated in Fig. 3(a) whereas the direct projectile-nucleus scattering largely decides the recoil peak, as seen in Fig. 3(b). The smaller binary and recoil peaks observed in Fig. 3(b) and Fig. 3(a), respectively, are due to successive two-body scatterings contained in the final-state wave functions. Although there are differences in the shape of the scattering amplitudes within the models $\mathcal{A}=\mathcal{A}^c$ and $\mathcal{A}=\mathbb{1}$, the decisive role of the three-body coupling is the different weighting of these individual amplitudes which leads to completely different interference [compare Figs. 2(a)–2(c)]. Hence, from this and previous analysis [20] we come to the conclusion that structures in the individual, incoherent scattering amplitudes can still be traced to two-body scattering processes even at lower energies. The observed cross sections, however, are determined by the interference pattern of these amplitudes which is decided by three-body coupling. This conclusion is consistent with the intuitive physical picture that three-body interactions are more significant at low relative velocities of the collision partners whereas their effect is expected to decline at higher velocities since, as we have shown, in the former case interference effects largely decide the calculated quantities. This theoretical study has been confirmed by further experimental data in a different kinematical arrangement [19]. It should be emphasized that the above analysis can be carried out for arbitrary (nonrelativistic) scattering reactions leading to three-charged particles above the complete dissociation threshold. The task lies, however, in determining the matrix $\mathcal{A}^c$ for the reaction under consideration.

In conclusion, a method for separating effects due to two-body interactions from those originating from three-body coupling is proposed and applied to the analysis of electron-impact ionization of atomic hydrogen in the low-velocity, coplanar, asymmetric energy-sharing kinematic. It has been shown that three-body interactions largely decide the weighting of individual scattering amplitudes, and hence, the interference pattern between these amplitudes. As this interference becomes less important at higher velocities the effect of three-body coupling declines in this region.

I would like to thank Jochen Röder for communicating his data prior to publication. I am grateful to John S. Briggs for many discussions on this subject. I also would like to thank Steve Buckman and Erich Weigold for helpful suggestions and comments. This work was supported by the Alexander von Humboldt Foundation and the Australian National University.

[1] L. H. Thomas, Proc. R. Soc. London Ser. A **114**, 561 (1927).
[2] R. Shakschaft and J. M. Wadehra, Phys. Rev. A **22**, 968 (1980).
[3] R. Shakschaft and L. Spruch, Rev. Mod. Phys. **51**, 396 (1979).
[4] E. Horsdal-Pedersen, C. L. Locke, and M. Stöckli, Phys. Rev. Lett. **50**, 1910 (1983).
[5] J. H. McGuire, Phys. Rev. Lett. **49**, 1153 (1982).
[6] J. S. Briggs, J. Phys. B **19**, 703 (1986).
[7] J. S. Briggs, T. Greenland, and L. Kocbach J. Phys. B. **15**, 3085 (1983).
[8] F. W. Byron, Jr. and C. J. Joachain, Phys. Rep. **179**, 211 (1989).
[9] J. Berakdar and H. Klar, J. Phys. B. **26**, 4219 (1993).
[10] H. Ehrhardt, K. Jung, G. Knoth, and P. Schlemmer, Z. Phys. D **1**, 3 (1986).
[11] B. Lohmann, I.E. McCarthy, A. T. Stelbovics, and E. Weigold, Phys. Rev. A **30**, 758 (1984).
[12] I. E. McCarthy and E. Weigold, Rep. Prog. Phys. **54**, 781 (1991).
[13] J. Berakdar, in *(e,2e) & Related Processes,* edited by C. T. Whelan, H. R. J. Walters, A. Lahmam-Bennani, and H. Ehrhardt, Vol. 44 of *NATO Advanced Study Institute Series C: Mathematical & Physical Sciences* (Kluwer Academic Press, New York, 1993), p. 131ff.
[14] H. R. J. Walters, Phys. Rep. **116**, 1 (1984).
[15] C. T. Whelan, R. J. Allan, J. Rasch, H. R. J. Walters, X. Zhang, J. Röder, K. Jung, and H. Ehrhardt, Phys. Rev. A **50**(5), 4394 (1994).
[16] J. Berakdar, Phys. Rev. A **53**, 2314 (1996).
[17] G. Wannier, Phys. Rev. **90**, 817 (1953).
[18] J. Berakdar, Aust. J. Phys. **49**, 1095 (1996).
[19] J. Berakdar, J. Röder, J.S. Briggs, and H. Ehrhardt, J. Phys. B (to be published).
[20] J. Berakdar and J. S. Briggs, J. Phys. B **27**, 4271 (1994).
[21] J. Röder (private communication).